Neuronal migration is mediated by inositol hexakisphosphate kinase 1 via α-actinin and focal adhesion kinase

Chenglai Fu[a], Jing Xu[a], Weiwei Cheng[b], Tomas Rojas[a], Alfred C. Chin[a], Adele M. Snowman[a], Maged M. Harraz[a], and Solomon H. Snyder[a,c,d,1]

[a]The Solomon H. Snyder Department of Neuroscience, Johns Hopkins University School of Medicine, Baltimore, MD 21205; [b]Division of Neuropathology, Department of Pathology, Johns Hopkins University School of Medicine, Baltimore, MD 21205; [c]Department of Pharmacology and Molecular Sciences, Johns Hopkins University School of Medicine, Baltimore, MD 21205; and [d]Department of Psychiatry and Behavioral Sciences, Johns Hopkins University School of Medicine, Baltimore, MD 21205

Contributed by Solomon H. Snyder, January 6, 2017 (sent for review October 26, 2016; reviewed by Per-Olof Berggren and Stephen B. Shears)

Inositol hexakisphosphate kinase 1 (IP6K1), which generates 5-diphosphoinositol pentakisphosphate (5-IP7), physiologically mediates numerous functions. We report that *IP6K1* deletion leads to brain malformation and abnormalities of neuronal migration. IP6K1 physiologically associates with α-actinin and localizes to focal adhesions. *IP6K1* deletion disrupts α-actinin's intracellular localization and function. The *IP6K1* deleted cells display substantial decreases of stress fiber formation and impaired cell migration and spreading. Regulation of α-actinin by IP6K1 requires its kinase activity. Deletion of *IP6K1* abolishes α-actinin tyrosine phosphorylation, which is known to be regulated by focal adhesion kinase (FAK). FAK phosphorylation is substantially decreased in *IP6K1* deleted cells. 5-IP7, a product of IP6K1, promotes FAK autophosphorylation. Pharmacologic inhibition of IP6K by TNP [N2-(*m*-Trifluorobenzyl), N6-(*p*-nitrobenzyl)purine] recapitulates the phenotype of *IP6K1* deletion. These findings establish that IP6K1 physiologically regulates neuronal migration by binding to α-actinin and influencing phosphorylation of both FAK and α-actinin through its product 5-IP7.

IP6K | inositol pyrophosphate | brain malformation | actinin | FAK

Inositol phosphates are prominent signaling molecules of which inositol 1, 4, 5-trisphosphate (IP3) is best characterized as a major second messenger acting by the release of intracellular calcium. Higher inositol polyphosphates have been increasingly appreciated, especially diphosphoinositol pentakisphosphate (IP7), which incorporates an energetic pyrophosphate bond (1). The biosynthesis of IP7 is mediated by a family of three inositol hexakisphosphate kinases (IP6K) on the 5-position or by Vip1/PPIP5K (PP-InsP5 kinase) family on the 1-position of the inositol ring (2–6). Thus, cells possess two IP7 isomers, 5-IP7 and 1-IP7, which differ in whether the 5- or 1-position is diphosphorylated. IP8 (1,5PP2-IP4) is formed when both the 5- and 1- positions are diphosphorylated (6). IP7 mediates several physiological functions. For instance, 5-IP7 is required for insulin secretion (7), and both 5-IP7 and 1-IP7 regulate PIP3 signaling pathways (8). The three IP6Ks generate a single isomer of 5-IP7 whose pyrophosphate bond occurs at C-5, but which arise from distinct genes and mediate diverse functions. For instance, IP6K3 regulates the neuronal cytoskeleton via interactions with adducin/spectrin (5). *IP6K1* deletion leads to sterility in males as well as resistance to diabetes and augmented Akt signaling (3). IP6K2 influences cell death, being required for apoptosis associated with p53 (9) and impacting migration and metastasis of tumor cells (4).

α-Actinin is an abundant cytoskeletal protein best known for its ability to cross-link actin filaments. α-Actinin is a major determinant of stress fibers, stabilizing them and enhancing their ability to generate tension (10, 11). α-Actinin also binds integrins, influences cellular adhesions, and is required for migration and spreading of many cell types (12, 13). α-Actinin is tyrosine-phosphorylated by focal adhesion kinase (FAK), which regulates actin stress fiber formation (14, 15). FAK plays a critical role in neuronal development, deficiency of which results in delays of neuronal migration (16) and brain abnormalities (17).

Bhandari and coworkers (18) reported a role for IP6K1 in cell migration and invasion, analogous to comparable functions of IP6K2 (4). *IP6K1*-deficient cells manifest defects in adhesion-dependent signaling with reduced activation of FAK and paxillin as well as diminished cell spreading and migration. Such defects are rescued by catalytically active but not inactive IP6K1.

In this study, we investigated neural phenotypes of *IP6K1* deletion. We have identified notable defects in neuronal migration associated with layering of the cerebral cortex. In seeking molecular concomitants, we observed selective binding of IP6K1 to α-actinin. Deletion of *IP6K1* or inhibiting its catalytic activity pharmacologically disrupts cell migration. Loss of IP6K1 leads to major defects in the disposition of FAK and its downstream targets.

Results

Defects in Neural Structure and Neuronal Migration Associated with *IP6K1* Deletion. We observe premature death in *IP6K1*-deleted mice (Fig. S1). Thus, whereas the proportion of wild-type (WT) and *IP6K1* deleted fetuses does not differ, among adults, numbers of *IP6K1* knockouts are reduced by approximately 40% (Fig. S1).

To assess the role of IP6K1 in neuronal development, we examined the brain structure of mutant mice by immunostaining the endogenous proteins. The morphology of the cerebral cortex is altered in *IP6K1* mutants at postnatal day 0 (P0), P7, and at 8 wk of age (Fig. 1). Cysts are observed throughout the cerebral cortex in layers 2–4, identified by Satb2 staining, and in layer 5, monitored by Ctip2. The abnormal cyst-like structures are evident at all time points examined from P0 to P7 and at 8 wk of

Significance

Inositol hexakisphosphate kinase 1 (IP6K1) regulates numerous physiological functions. We describe a role of IP6K1 in neural development, because its deletion results in defects in neuronal migration and brain malformation. IP6K1 physiologically interacts with α-actinin and localizes to focal adhesions. IP6K1 regulates phosphorylation of both focal adhesion kinase and α-actinin through its product 5-diphosphoinositol pentakisphosphate (5-IP7).

Author contributions: C.F. and S.H.S. designed research; C.F., J.X., W.C., T.R., A.C.C., A.M.S., and M.M.H. performed research; C.F., J.X., W.C., T.R., A.C.C., A.M.S., M.M.H., and S.H.S. analyzed data; and C.F. and S.H.S. wrote the paper.

Reviewers: P.-O.B., Karolinska Institutet; and S.B.S., National Institute of Environmental Health Sciences.

The authors declare no conflict of interest.

[1]To whom correspondence should be addressed. Email: ssnyder@jhmi.edu.

This article contains supporting information online at www.pnas.org/lookup/suppl/doi:10.1073/pnas.1700165114/-/DCSupplemental.

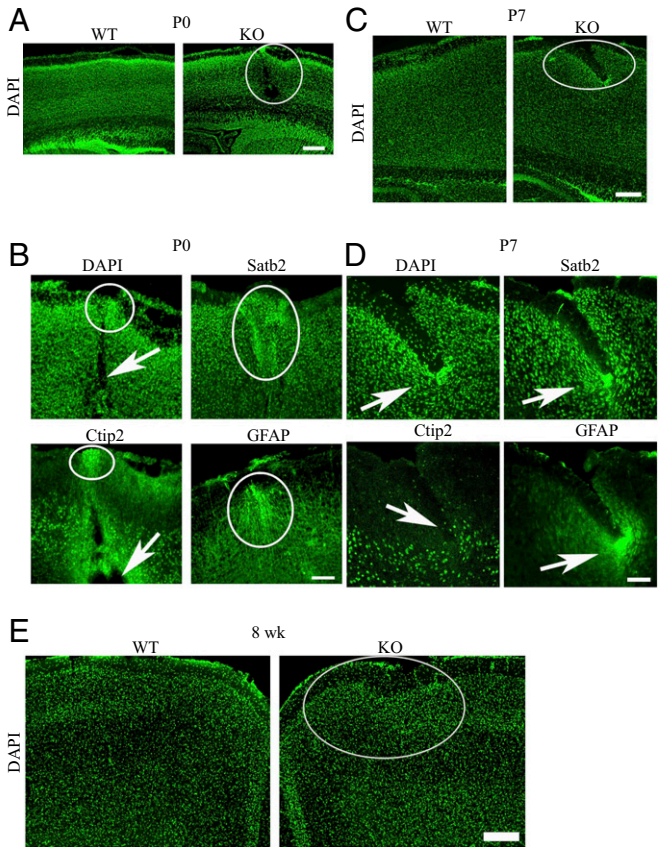

Fig. 1. *IP6K1* deletion is associated with brain malformation. (*A*) DAPI staining of the sagittal sections of P0 WT and *IP6K1* KO mice brains. The *IP6K1* KO cerebral cortex shows cysts inside the cortex and indentation at the superficial layer (circle). ($n = 3$). (*B*) Immunostaining of the sagittal sections of P0 *IP6K1* KO cerebral cortex with DAPI, anti-Satb2 (staining cortical layer 2–4), anti-Ctip2 (staining cortical layer 5) and anti-GFAP (staining glial cells) antibodies. Abnormal aggregations of Satb2-positive neurons and GFAP-positive glial cells occur at the superficial brain layers of the *IP6K1* KOs' (circle); arrows point to the cysts. ($n = 3$). (*C*) DAPI staining of the sagittal sections of P7 WT and *IP6K1* KO mice brains. The KO cortex reveals abnormal sulci (circle). ($n = 3$). (*D*) Immunostaining of the sagittal sections of P7 *IP6K1* KO cerebral cortex with DAPI, anti-Satb2, anti-Ctip2 and anti-GFAP antibodies. Abnormal aggregations of Satb2-positive neurons and GFAP-positive glial cells surround the sulcus (arrow). ($n = 3$). (*E*) DAPI staining of coronal sections of 8-wk WT and *IP6K1* KO mice brains. *IP6K1* deleted cortex shows curved neuron layers (circle). ($n = 3$). (Scale bars: *A*, *C*, and *E*, 200 μm; *B* and *D*, 100 μm.)

age. The disposition of the cysts and closely surrounding cells is similar whether stained by Satb2 and Ctip2, which are selective for neurons, or GFAP, which uniquely labels glia.

To determine whether the aberrant neural disposition of *IP6K1* knockouts reflects abnormalities of development, we monitored neuronal disposition at embryonic day 15 (E15) following the administration of EdU (5-ethynyl-2'-deoxyuridine) 4, 24, 48, and 72 h before analysis of brain tissue (Fig. 2 *A*–*E*). Retardation of neuronal migration is first evident in *IP6K1* mutants at 24 h after EdU administration and persists at 48 and 72 h.

We evaluated the comparative movement of different layers at E17 via staining the endogenous Satb2 and Ctip2 for layers 2–4 and 5, respectively (Fig. 2*F*). In WT preparations at E17, Satb2 and Ctip2 appear to have attained their adult sites, whereas in the *IP6K1* knockouts, migration of Satb2 and Ctip2 continues. Similarly, at P0 and P7, Satb2/Ctip2 in WT mice are in adult sites, whereas migration appears to still be taking place for the *IP6K1* knockouts (Fig. 2 *G* and *H*).

In summary, *IP6K1* deletion is associated with a substantial retardation of neuronal migration in embryonic and early postnatal life.

IP6K1 Interacts with α-Actinin. We wondered whether the abnormalities of neuronal migration in *IP6K1* mutants might reflect alterations of IP6K1 interactions with selected proteins. Accordingly, we immunoprecipitated IP6K1 and investigated its interacting proteins. Immunoprecipitation with antibodies to IP6K1 results in the pull-down of numerous proteins. Of these proteins, only a few are lost in *IP6K1* knockouts (Fig. 3*A*). Presumably such deleted bands reflect proteins that physiologically bind IP6K1. A prominent band that binds IP6K1 is identified as α-actinin (Fig. 3*A*). We confirmed IP6K1/α-actinin binding by

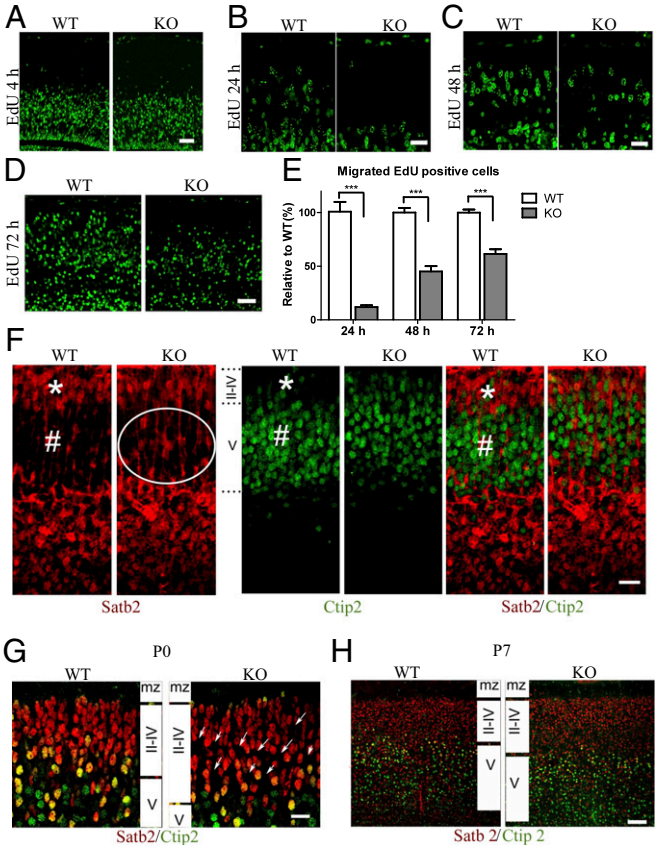

Fig. 2. *IP6K1* deletion results in neuronal migration deficiency. (*A*–*E*) EdU was injected to pregnant heterozygous mice at E15; the brain slices of the littermate fetuses were processed 4, 24, 48, and 72 h later. (*A*) No EdU-positive cells are observed in the brain superficial layers at 4 h ($n = 3$). (*B*) At 24 h, many EdU-positive cells have reached the top layers in the WT brains, whereas few EdU-positive cells have migrated to the top layers in the *IP6K1* KO brains. ($n = 3$). (*C*) Substantially less EdU-positive cells have migrated to the brain's top layers in the *IP6K1* KOs at 48 h. ($n = 3$). (*D*) Significantly less EdU-positive cells have migrated to the brain's top layers in the *IP6K1* KOs at 72 h. ($n = 3$). (*E*) Statistic analysis of the migrated EdU-positive cells at 24, 48, and 72 h after injection. Data are presented as means ± SEM ($n = 3$). ***$P < 0.001$, Student's t test. (*F*) Littermates of E17 WT and *IP6K1* KO brains were cut sagittally and stained by labeling with Satb2 for layers 2–4 and Ctip2 for layer 5. In WT preparations the Satb2-positive cells have reached the top layers and separated from the Ctip2-positive neurons to form a clear layer. However, in the KOs the Satb2-positive neurons have not fully migrated to the top layers (circle), and have not separated from the Ctip2-positive neurons. (*, layer 2–4; #, layer 5; $n = 3$). (*G*) The P0 WT and *IP6K1* KO brains were cut sagittally and stained for Satb2 and Ctip2. The distance between neurons is significantly longer in the KOs (arrows). ($n = 3$). (*H*) P7 WT and *IP6K1* KO brains were cut sagittally and stained for Satb2 and Ctip2. The distance between neurons is substantially longer in the KOs. ($n = 3$). (Scale bars: *A*, *D*, and *G*, 50 μm; *B*, *C*, and *F*, 20 μm; *H*, 100 μm.)

NEUROSCIENCE

immunoprecipitation of IP6K1, which reveals binding to α-actinin in WT preparations but not in *IP6K1* knockouts (Fig. 3*B*). We explored IP6K1/α-actinin binding in vitro by using bacterially generated proteins (Fig. 3 *C–E*). IP6K1 binds robustly to α-actinin in vitro as does the catalytically inactive IP6K1 (K226A). Thus, binding of the two proteins does not depend on IP6K1 catalytic activity.

We stained endogenous IP6K1 and α-actinin in HeLa cells in which the two proteins colocalize on the cell membrane (Fig. S2*A*). We then studied the colocalization of endogenous IP6K1 with FAK by immunostaining in HeLa cells (Fig. S2*B*). IP6K1 and FAK colocalize in focal adhesions. We further established the selectivity of α-actinin/IP6K1 binding by comparing its interactions with those of IP6K1 and other proteins associated with focal adhesion such as vinculin, FAK, and paxillin (Fig. 3 *F* and *G*). Pull-down of IP6K1 coprecipitates α-actinin but not vinculin, paxillin, or FAK, indicating that IP6K1 does not bind to FAK directly.

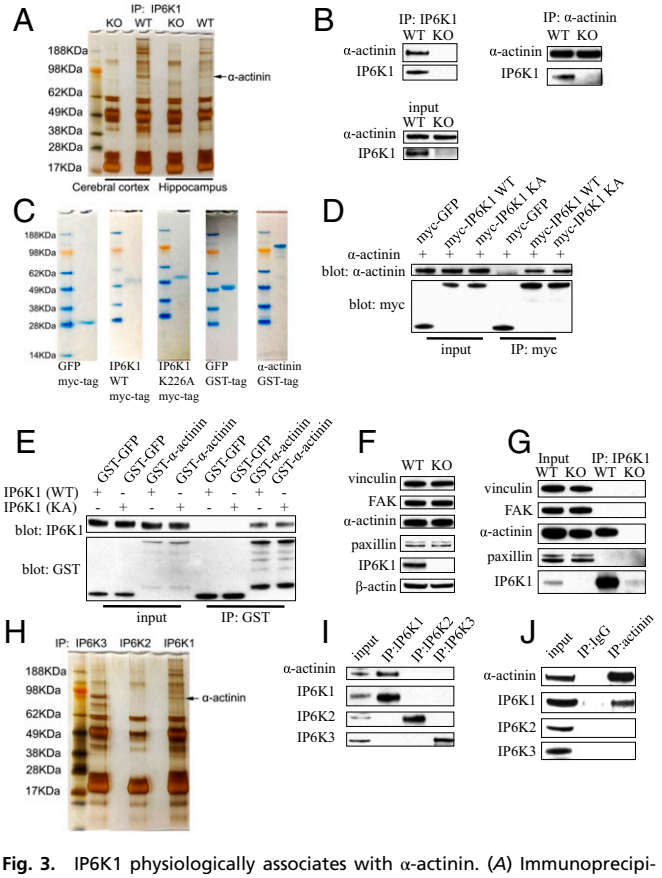

Fig. 3. IP6K1 physiologically associates with α-actinin. (*A*) Immunoprecipitation of IP6K1 from WT and *IP6K1* KO cerebral cortex and hippocampus; silver staining and mass spectrometry reveals α-actinin coprecipitated by IP6K1. (*B*) Immunoprecipitation of IP6K1 or α-actinin from WT and *IP6K1* KO brains; Western blot shows the binding of IP6K1 with α-actinin. (*C*) In vitro expression of myc-tag GFP, myc-tag IP6K1 (WT), myc-tag IP6K1 (K226A), GST-tag GFP, and GST-tag α-actinin. (*D* and *E*) In vitro binding of IP6K1 and α-actinin. (*D*) Immunoprecipitation of myc tag. Western blot shows α-actinin pulled down by both WT and K226A mutant IP6K1. (*E*) Immunoprecipitation of GST tag. Western blot reveals both WT and K226A mutant IP6K1 are coprecipitated by α-actinin. (*F*) Western blot shows the expression levels of vinculin, FAK, α-actinin, and paxillin do not change in the *IP6K1* KO brains. (*G*) Immunoprecipitation of IP6K1 from WT and *IP6K1* KO brains. Western blot shows IP6K1 binds with α-actinin but not vinculin, FAK, or paxillin. (*H*) Immunoprecipitation of IP6K1, 2, and 3 from WT mouse brain. Silver stain reveals α-actinin binds only with IP6K1. (*I*) Immunoprecipitation of IP6K1, 2, and 3 from WT mouse brain. Western blot shows α-actinin binds only with IP6K1. (*J*) Immunoprecipitation of α-actinin or control IgG from WT mouse brain. Western blot demonstrates α-actinin interacts only with IP6K1.

The IP6K1–α-actinin interaction is unique for IP6K1. Thus, immunoprecipitation with antibodies to IP6K2 and IP6K3 fails to coprecipitate α-actinin in experiments wherein IP6K1 antibodies robustly pull down α-actinin (Fig. 3 *H–J*).

Disruption of IP6K1/α-Actinin Interactions Leads to Abnormalities of Cell Motility. We wondered whether loss of IP6K1 influences the cellular disposition of α-actinin. We examined the endogenous localization of α-actinin in *IP6K1*-deleted mouse embryonic fibroblasts (MEFs) (Fig. 4*A*). In WT MEFs, α-actinin is selectively associated with cellular membranes, especially the plasma membrane, whereas in *IP6K1* knockout cells, α-actinin is widely dispersed throughout the cell (Fig. 4*A*).

α-Actinin coordinates the disposition of actin in stress fibers (11). We examined stress fibers in *IP6K1*-deleted MEFs (Fig. 4*B*). The normal patterns of stress fibers are markedly disrupted in *IP6K1* knockouts, indicating an important role for this enzyme in stress fiber formation and function.

The focal adhesion system mediates cellular migration and spreading (19). We evaluated these processes in a variety of models. In the scratch assay in MEFs, *IP6K1* knockout elicits a 30% decrease in movement (Fig. 4*C*). The Boyden chamber assay reveals a 50% decline of cellular motility in the mutant preparations (Fig. 4*D*). We monitored spreading of MEFs, a process that is diminished by approximately 55% in *IP6K1* knockouts (Fig. 4*E*). The formation of stress fibers is also disrupted in IP6K1-deleted MEFs plated on fibronectin (Fig. 4*F*).

We rescued abnormalities in *IP6K1* knockouts by overexpressing WT IP6K1 or catalytically inactive IP6K1-kinase dead (KD) (Fig. 4 *G–J*). The dispersal of α-actinin staining in the *IP6K1* knockouts is reversed by overexpressing WT IP6K1 but not IP6K1-KD (Fig. 4*G*). Likewise, the formation of actin stress fibers is normalized by WT IP6K1 but not the kinase-deficient mutant (Fig. 4*H*). Thus, catalytic activity of IP6K1 is required for its ability to enhance the functions of α-actinin. Similarly, in a scratch assay for cellular motility (Fig. 4*I* and Fig. S3*A*) and in the Boyden chamber assay (Fig. 4*J* and Fig. S3*B*), the defect of *IP6K1* knockouts in motility is reversed by WT IP6K1 but not by a catalytically dead mutant.

The kinase activity is also required for cell spreading (Fig. S3*C*). Thus, WT IP6K1, but not the kinase dead mutant, rescues cell spread.

Pharmacologic Inhibition of IP6 Kinase Impacts Cellular Motility Similar to *IP6K1* Deletion. We sought pharmacologic approaches to complement genetic evidence for a role of inositol phosphate kinase activity in neuronal migration (Fig. 5). TNP [N2-(*m*-Trifluorobenzyl), N6-(*p*-nitrobenzyl)purine] is a potent and fairly selective inhibitor of IP6Ks (20). We tested the cytotoxicity of TNP on HeLa cells (Fig. S4), TNP up to 10 μM does not affect cell viability. We examined the influence of TNP (10 μM) upon the disposition of α-actinin and cell migration. In HeLa cells, TNP markedly disrupts the normal membranous localizations of endogenous α-actinin (Fig. 5*A*). TNP treatment also recapitulates the abnormalities of F-actin disposition in HeLa cells that are associated with *IP6K1* deletion (Fig. 5*B*). Similarly, abnormalities of cell movement observed in *IP6K1* mutants by scratch assay, Boyden chamber assay, and spreading assays are also evident with TNP treatment (Fig. 5 *C–E* and Fig. S5).

Tyrosine Phosphorylation of α-Actinin Is Abnormal in Preparations Deficient in *IP6K1*. 5-IP7 is reported to phosphorylate target proteins (21, 22), which is exclusively on serine. However, neither IP6K1 deletion nor TNP treatment alters α-actinin phosphoserine/threonine (Fig. S6). Thus, 5-IP7 may not phosphorylate α-actinin directly. Tyrosine phosphorylation of α-actinin is required for its normal functions (14, 15). *IP6K1* knockout leads to virtual abolition of α-actinin tyrosine-phosphorylation in the

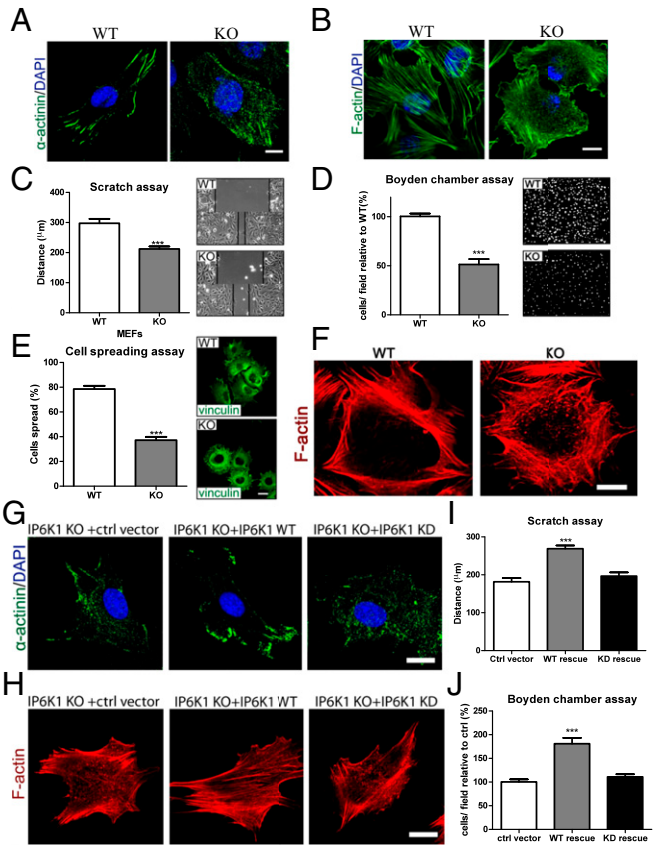

Fig. 4. *IP6K1* deletion disrupts α-actinin function and cell migration. (*A*) Immunostaining of α-actinin in WT and *IP6K1* KO MEFs. *IP6K1* deletion disrupts α-actinin's intracellular localization, resulting in diffuse dispersal of α-actinin in the KO cells. (*B*) Immunostaining of F-actin in WT and *IP6K1* KO MEFs. Actin stress fibers are poorly developed in the KO cells. (*C*) The scratch migration assay shows significantly migration delay of the *IP6K1* KO MEFs. Data are presented as means ± SEM ($n = 4$). ***$P < 0.001$, Student's t test. (*D*) The Boyden chamber migration assay demonstrates substantially migration deficits in *IP6K1*-deleted MEFs. Data are presented as means ± SEM ($n = 4$). ***$P < 0.001$, Student's t test. (*E* and *F*) WT and *IP6K1* KO MEFs were seeded onto fibronectin-coated plates for spreading assay for 1 h. (*E*) The spreading cells were stained for vinculin. The percentage of spread cells was calculated. Significantly fewer cells spread when *IP6K1* is deleted. Data are presented as means ± SEM ($n = 4$). ***$P < 0.001$, Student's t test. (*F*) F-actin staining demonstrates defective actin stress fiber formation in the KO cells. (*G*–*J*) *IP6K1* KO MEF cells were rescued by control vector, WT IP6K1, or KD IP6K1. (*G*) Immunostaining of α-actinin. The natural localization of α-actinin is rescued only by WT IP6K1. (*H*) Immunostaining of F-actin. The actin stress fiber formation is rescued only by WT IP6K1. (*I*) The scratch migration assay shows cell migration can only be rescued by WT IP6K1. Data are presented as means ± SEM ($n = 4$). ***$P < 0.001$, Student's t test. (*J*) The Boyden chamber assay demonstrates that migration is rescued only by WT IP6K1. Data are presented as means ± SEM ($n = 4$). ***$P <$ 0.001, Student's t test. (Scale bars: *A*, *B*, and *F*–*H*, 10 μm; *E*, 20 μm.)

brain (Fig. 5*F*). Similarly, TNP treatment of HeLa cells markedly diminishes tyrosine phosphorylation of α-actinin (Fig. 5*G*). However, 5-IP7 does not directly phosphorylate α-actinin on tyrosine in an in vitro preparation (Fig. S6*C*).

We evaluated enzymatic systems that might mediate α-actinin tyrosine phosphorylation. α-Actinin is known to be tyrosine-phosphorylated by focal adhesion kinase (FAK) (14). Fibronectin treatment of MEFs elicits robust phosphorylation of FAK at Y397, Y576/577, and Y925. This treatment also leads to substantial tyrosine phosphorylation of paxillin (Fig. 5*H*). Phosphorylation of each of these proteins is markedly diminished in *IP6K1*-deleted preparations.

We substantiated these results by knocking down *IP6K1* with shRNA in HeLa cells (Fig. 5*I*). Fibronectin's enhancement of phospho-FAK Y397, Y576/577, and Y925 is markedly diminished by down-regulation of *IP6K1*.

IP6K1 Activity Promotes Focal Adhesion Kinase Activity. We established that phosphorylation of FAK is determined by IP6K1 (Fig. 6 *A* and *B*). Thus, phosphorylation of FAK is diminished approximately 70% in *IP6K1*-deleted MEFs. Staining with vinculin confirms the association of endogenous phospho-FAK with focal adhesions. *IP6K1* knockout provides a 65–70% diminution of phospho-FAK-Y397 staining. Phospho-paxillin, a target of FAK, is similarly diminished in *IP6K1* knockouts (Fig. 6 *C* and *D*).

Catalytic activity of IP6K1 is required for regulation of FAK phosphorylation. Thus, the diminished FAK phosphorylation of

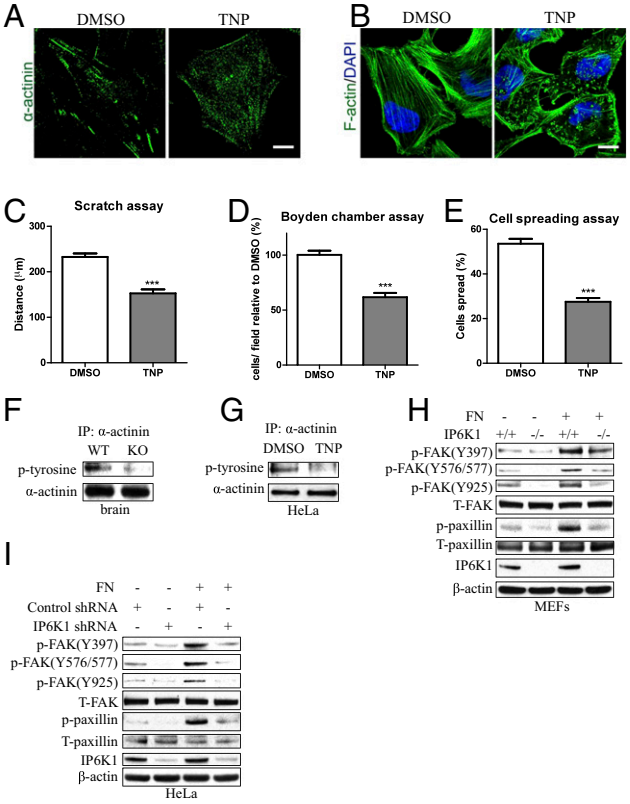

Fig. 5. Inhibition of IP6 kinase activity disrupts α-actinin. (*A* and *B*) HeLa cells were treated with DMSO or TNP (10 μM for 24 h). (*A*) Immunostaining of α-actinin. TNP treatment disturbs α-actinin localization. (*B*) F-actin was labeled by phalloidin. TNP treatment markedly inhibits the actin stress fiber formation. (*C* and *D*) TNP (10 μM for 24 h) treatment significantly impedes cell migration, demonstrated by scratch assay (*C*) and Boyden chamber assay (*D*). Data are presented as means ± SEM ($n = 4$). ***$P < 0.001$, Student's t test. (*E*) TNP (10 μM for 24 h) treatment substantially inhibits cell spreading. Data are presented as means ± SEM ($n = 4$). ***$P < 0.001$, Student's t test. (*F*) Immunoprecipitation of α-actinin from WT or *IP6K1* KO brains. Western blot shows significantly decreased tyrosine phosphorylation of α-actinin in the *IP6K1* KOs. (*G*) Immunoprecipitation of α-actinin from DMSO or TNP (10 μM for 24 h) treated HeLa cells. Western blot demonstrates that TNP treatment blocks tyrosine phosphorylation of α-actinin. (*H*) WT and *IP6K1* KO MEFs were planted onto cell culture plates (coated with or without fibronectin) for 30 min. Western blot shows that phosphorylation of FAK and paxillin are drastically decreased in IP6K1 KOs. (*I*) *IP6K1* was depleted by shRNA transduction in HeLa cells. The control and *IP6K1*-deleted HeLa cells were planted onto cell culture plates (coated with or without fibronectin) for 30 min. Western blot demonstrates that *IP6K1* deletion blocks FAK phosphorylation. (Scale bars: 10 μm.)

NEUROSCIENCE

IP6K1 knockout MEFs is reversed by overexpressing WT IP6K1 but not the kinase-dead enzyme (Fig. 6*E*).

Pharmacologic support for the genetic data are provided by the use of TNP that dose-dependently diminishes all examined forms of tyrosine phosphorylation of FAK and paxillin (Fig. 6*F* and Fig. S7).

In findings similar to our own, Bhandari and coworkers (18) demonstrated decreases of FAK and paxillin activation in *IP6K1* mutants. Moreover, the FAK phosphorylation could be rescued by catalytically active but not inactive IP6K1.

5-IP7 Promotes Autophosphorylation of FAK. The requirement of IP6 kinase catalytic activity for regulation of FAK implies that an inositol phosphate product of IP6K1 plays a regulatory role. 5-IP7 is the principal product of IP6K1 catalytic activity (3). We examined phospho-tyrosine phosphorylation of FAK in vitro in the presence of IP6 or 5-IP7 (Fig. 6*G*). 5-IP7 but not IP6 markedly increases tyrosine phosphorylation of FAK. This phosphorylation is not affected by TNP, consistent with TNP acting selectively to inhibit the generation of 5-IP7 by IP6. Accordingly, one would not expect any influence of TNP in preparations in which 5-IP7 is already added. The potent and selective stimulation of FAK phosphorylation by 5-IP7 is consistent with the notion that regulation by IP6K1 of FAK phosphorylation is mediated by its generation of 5-IP7, which directly influences the autophosphorylation of FAK.

Thus, IP6K1 physiologically interacts with α-actinin and regulates both α-actinin and FAK phosphorylation through its product 5-IP7.

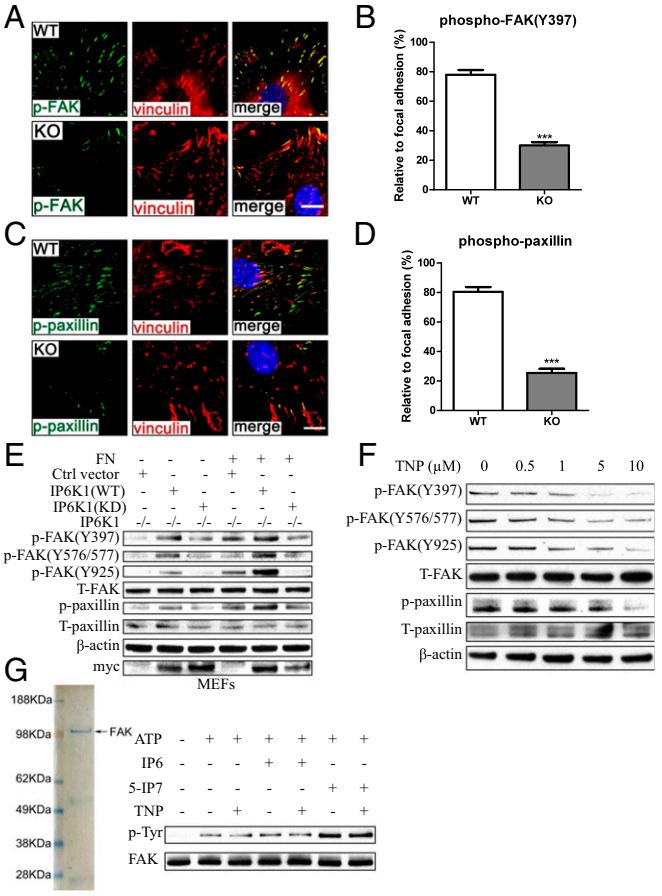

Fig. 6. IP6 kinase activity promotes FAK phosphorylation. (*A* and *B*) Immunostaining of phospho-FAK (Y397) and vinculin in WT and *IP6K1* KO MEFs. FAK phosphorylation is significantly decreased in *IP6K1* KOs. Data are presented as means ± SEM from 30 cells of three experiments. ***$P < 0.001$, Student's *t* test. (*C* and *D*) Immunostaining of phospho-paxillin and vinculin in WT and *IP6K1* KO MEFs. Paxillin phosphorylation is substantially decreased in *IP6K1*-deleted cells. Data are presented as means ± SEM from 30 cells of three experiments. ***$P < 0.001$, Student's *t* test. (*E*) *IP6K1* KO MEFs were rescued by control vector, WT IP6K1, or KD IP6K1. Cells were planted onto cell culture plates (coated with or without fibronectin) for 30 min. Western blot reveals that phosphorylation of FAK and paxillin is rescued only by WT IP6K1. (*F*) HeLa cells were treated with different concentrations of TNP for 24 h. TNP treatment dose dependently inhibits FAK phosphorylation. (*G*) FAK was expressed and purified from HEK293 cells. The in vitro autophosphorylation assay shows that 5-IP7 significantly promotes FAK phosphorylation. (Scale bars: 10 μm.)

Discussion

In this study, we investigated potential roles of IP6K1 in brain function by using *IP6K1*-deleted animals, which display major defects in neuronal migration. Explorations of IP6K1-binding proteins led to an appreciation of α-actinin as an important determinant of these processes. Specifically, IP6K1 binds α-actinin, which, in turn, interacts with FAK. These observations have culminated in elucidation of the following molecular scheme. In this model, IP6K1 binds to α-actinin, which brings it into proximity with FAK that, together with α-actinin, is part of the focal adhesion complex. 5-IP7 enhances autophosphorylation of FAK, which, in turn, augments neuronal migration.

Inositol phosphates have been associated with cell migration. Thus, earlier we reported that IP6K2, acting by the generation of 5-IP7, mediates cancer cell migration and metastasis both in cellular culture and in intact mice (4). In this process, IP6K2 augments adhesion to the cell matrix and decreases cell–cell adhesion. At a molecular level, this process involves the ability of 5-IP7 to cause nuclear sequestering and inactivation of the tumor suppressor enzyme liver kinase B 1. Earlier we reported that IP6K3 influences the formation of synapses in the brain (5). *IP6K3* knockout mice manifest aberrations in motor learning and coordination. Whether these influences, exerted notably on Purkinje cells of the cerebellum, are mediated by alterations in the movements of cells during neurogenesis is unclear.

It has been reported that 1-IP7 promotes the phosphorylation of IRF3, as does IP8, albeit less potently (23). In this study, we find that 5-IP7 promotes FAK phosphorylation. Both TNP and *IP6K1* deletion compromise the synthesis of 5-IP7 and IP8. There is a possibility that IP8 also enhances FAK autophosphorylation.

Our findings may have therapeutic ramifications. IP6K1 appears to mediate cellular motility. Increased movement of cell processes is a feature of malignancy. TNP inhibits all isoforms of IP6K and alters cellular disposition (20, 24, 25). It is possible that more potent and selective inhibitors of IP6K1 will have therapeutic benefit.

IP6K1 appears to regulate the disposition of stress fibers, which play a notable role in determining cell shape and function. Such actions of IP6K1 imply a fundamental role in determining overall cell structure and function.

Materials and Methods

Reagents. Chemicals were from Sigma-Aldrich. Antibodies are listed in *SI Materials and Methods*.

Animals. The WT and *IP6K1* KO animals were littermates from heterozygous breeding. Animal breeding and procedures were conducted in strict accordance with the NIH Guide for Care and Use of Laboratory Animals.

Immunofluorescence Staining. Immunofluorescence staining was performed as reported (26). The investigation conformed to the Guide for the Care and Use of Laboratory Animals published by the US National Institutes of Health.

EdU Labeling of Neuronal Migration. Heterozygous breeding pregnant mice at E15 were injected i.p. with 100 mg/kg EdU in normal saline and fetus were harvested at 4, 24, 48, or 72 h after injection. The fetus were fixed with 4% (wt/vol) paraformaldehyde and cut at sagittal sections. The slices were stained with Alexa Fluor 488 picolyl azide to label EdU-incorporated cells (Thermo Fisher Scientific).

Immunoblotting and Immunoprecipitation. Standard methods for cell lysis, immune precipitation, SDS/PAGE, and Western blot were applied (5).

Cell Culture and Lentiviral Transduction. WT and *IP6K1* KO MEF cells, HeLa cells, HEK293, and HEK293T cells were cultured in DMEM with 10% (vol/vol) FBS. Lentiviral production and transduction were generated as reported (27). *IP6K1* knock-down HEK293 cells were generated by lentiviral transduction and maintained in DMEM with 5 μg/mL puromycin.

In Vitro Protein Expression and Purification. The myc-tag GFP, myc-tag WT IP6K1, and myc-tag kinase-dead mutant IP6K1 (K226A) were cloned into the pGEX-6P-2 vector (GE Healthcare Life Sciences). PreScission Protease was used to remove the GST from myc-tag GFP, myc-tag WT, and K226A mutant IP6K1. GFP and α-actinin were also cloned into the pGEX-6P-2 vector (GE Healthcare Life Sciences) to produce GST-fused GFP and GST fused α-actinin (5).

Cell Migration and Spreading. The scratch migration assay and Boyden chamber assay were done as described (28).

5-IP7 Synthesis. The 5-IP7 was prepared as described (29). Incubating 100 ng of purified IP6K1 in 25 μL of reaction buffer containing 20 mM Tirs-HCl, pH 7.4, 50 mM NaCl, 6 mM $MgSO_4$, 1 mM DTT, 40 μg/mL BSA, 10 mM phosphocreatine, 10 U creatine phosphokinase, 1 mM ATP, and 400 μM IP6 at 37 °C overnight.

In Vitro Autophosphorylation. α-Actinin and flag-tag FAK was expressed and purified from HEK293 cells. The in vitro autophosphorylation assay was done by incubating α-actinin or FAK in reaction buffer (20 mM Hepes, pH 7.4, 5 mM $MgCl_2$, 5 mM $MnCl_2$), added with ATP (10 μM), IP6 (10 μM), 5-IP7 (10 μM), or TNP (10 μM) at 37 °C for 20 min (30).

Statistical Analysis. Quantitative data are expressed as means ± SEM. Data were analyzed by one-way ANOVA, unpaired Student's *t* test. $P < 0.05$ was considered statistically significant. For nonquantitative data, results were representative of at least three independent experiments.

ACKNOWLEDGMENTS. We thank all the members in the S.H.S. laboratory. This work was supported by US Public Health Service Grant DA000266 (to S.H.S.).

1. Voglmaier SM, et al. (1996) Purified inositol hexakisphosphate kinase is an ATP synthase: Diphosphoinositol pentakisphosphate as a high-energy phosphate donor. *Proc Natl Acad Sci USA* 93(9):4305–4310.
2. Mulugu S, et al. (2007) A conserved family of enzymes that phosphorylate inositol hexakisphosphate. *Science* 316(5821):106–109.
3. Bhandari R, Juluri KR, Resnick AC, Snyder SH (2008) Gene deletion of inositol hexakisphosphate kinase 1 reveals inositol pyrophosphate regulation of insulin secretion, growth, and spermiogenesis. *Proc Natl Acad Sci USA* 105(7):2349–2353.
4. Rao F, et al. (2015) Inositol pyrophosphates promote tumor growth and metastasis by antagonizing liver kinase B1. *Proc Natl Acad Sci USA* 112(6):1773–1778.
5. Fu C, et al. (2015) Inositol hexakisphosphate kinase-3 regulates the morphology and synapse formation of cerebellar purkinje cells via spectrin/adducin. *J Neurosci* 35(31): 11056–11067.
6. Shears SB, Baughman BM, Gu C, Nair VS, Wang H (October 17, 2016) The significance of the 1-kinase/1-phosphatase activities of the PPIP5K family. *Adv Biol Regul*, 10.1016/j.jbior.2016.10.003.
7. Illies C, et al. (2007) Requirement of inositol pyrophosphates for full exocytotic capacity in pancreatic beta cells. *Science* 318(5854):1299–1302.
8. Gokhale NA, Zaremba A, Janoshazi AK, Weaver JD, Shears SB (2013) PPIP5K1 modulates ligand competition between diphosphoinositol polyphosphates and PtdIns (3,4,5)P3 for polyphosphoinositide-binding domains. *Biochem J* 453(3):413–426.
9. Rao F, et al. (2014) Inositol pyrophosphates mediate the DNA-PK/ATM-p53 cell death pathway by regulating CK2 phosphorylation of Tti1/Tel2. *Mol Cell* 54(1):119–132.
10. Foley KS, Young PW (2014) The non-muscle functions of actinins: An update. *Biochem J* 459(1):1–13.
11. Pavalko FM, Burridge K (1991) Disruption of the actin cytoskeleton after microinjection of proteolytic fragments of alpha-actinin. *J Cell Biol* 114(3):481–491.
12. Otey CA, Pavalko FM, Burridge K (1990) An interaction between alpha-actinin and the beta 1 integrin subunit in vitro. *J Cell Biol* 111(2):721–729.
13. Choi CK, et al. (2008) Actin and alpha-actinin orchestrate the assembly and maturation of nascent adhesions in a myosin II motor-independent manner. *Nat Cell Biol* 10(9):1039–1050.
14. Izaguirre G, et al. (2001) The cytoskeletal/non-muscle isoform of alpha-actinin is phosphorylated on its actin-binding domain by the focal adhesion kinase. *J Biol Chem* 276(31):28676–28685.
15. Feng Y, et al. (2013) α-actinin1 and 4 tyrosine phosphorylation is critical for stress fiber establishment, maintenance and focal adhesion maturation. *Exp Cell Res* 319(8): 1124–1135.
16. Valiente M, Ciceri G, Rico B, Marín O (2011) Focal adhesion kinase modulates radial glia-dependent neuronal migration through connexin-26. *J Neurosci* 31(32): 11678–11691.
17. Beggs HE, et al. (2003) FAK deficiency in cells contributing to the basal lamina results in cortical abnormalities resembling congenital muscular dystrophies. *Neuron* 40(3): 501–514.
18. Jadav RS, et al. (2016) Deletion of inositol hexakisphosphate kinase 1 (IP6K1) reduces cell migration and invasion, conferring protection from aerodigestive tract carcinoma in mice. *Cell Signal* 28(8):1124–1136.
19. Carragher NO, Frame MC (2004) Focal adhesion and actin dynamics: A place where kinases and proteases meet to promote invasion. *Trends Cell Biol* 14(5):241–249.
20. Padmanabhan U, Dollins DE, Fridy PC, York JD, Downes CP (2009) Characterization of a selective inhibitor of inositol hexakisphosphate kinases: Use in defining biological roles and metabolic relationships of inositol pyrophosphates. *J Biol Chem* 284(16): 10571–10582.
21. Saiardi A, Bhandari R, Resnick AC, Snowman AM, Snyder SH (2004) Phosphorylation of proteins by inositol pyrophosphates. *Science* 306(5704):2101–2105.
22. Bhandari R, et al. (2007) Protein pyrophosphorylation by inositol pyrophosphates is a posttranslational event. *Proc Natl Acad Sci USA* 104(39):15305–15310.
23. Pulloor NK, et al. (2014) Human genome-wide RNAi screen identifies an essential role for inositol pyrophosphates in Type-I interferon response. *PLoS Pathog* 10(2): e1003981.
24. Ghoshal S, et al. (2016) TNP [N2-(m-Trifluorobenzyl), N6-(p-nitrobenzyl)purine] ameliorates diet induced obesity and insulin resistance via inhibition of the IP6K1 pathway. *Mol Metab* 5(10):903–917.
25. Zhang Z, et al. (2014) Selective inhibition of inositol hexakisphosphate kinases (IP6Ks) enhances mesenchymal stem cell engraftment and improves therapeutic efficacy for myocardial infarction. *Basic Res Cardiol* 109(4):417.
26. Fu C, He J, Li C, Shyy JY, Zhu Y (2010) Cholesterol increases adhesion of monocytes to endothelium by moving adhesion molecules out of caveolae. *Biochim Biophys Acta* 1801(7):702–710.
27. Fu C, et al. (2013) Screening assay for blood vessel maturation inhibitors. *Biochem Biophys Res Commun* 438(2):364–369.
28. Zhu Z, et al. (2011) Prostaglandin E2 promotes endothelial differentiation from bone marrow-derived cells through AMPK activation. *PLoS One* 6(8):e23554.
29. Azevedo C, Burton A, Bennett M, Onnebo SM, Saiardi A (2010) Synthesis of InsP7 by the Inositol Hexakisphosphate Kinase 1 (IP6K1). *Methods Mol Biol* 645:73–85.
30. Burgaya F, et al. (1997) Alternatively spliced focal adhesion kinase in rat brain with increased autophosphorylation activity. *J Biol Chem* 272(45):28720–28725.